JOURNAL OF Applied Polymer SCIENCE

Synthesis and Characterization of Biodegradable Polyurethanes Based on L-Cystine/Cysteine and Poly(ε-caprolactone)

Jing Wang,[1] Zhen Zheng,[1] Quan Wang,[2] Pengfei Du,[1] Jinjun Shi,[1] Xinling Wang[1]

[1]School of Chemistry and Chemical Engineering, State Key Laboratory of Metal Matrix Composites, Shanghai Jiao Tong University, Shanghai 200240, People's Republic of China

[2]Chinese Academy of Agricultural Sciences, Shanghai Veterinary Research Institute, CAAS, Minhang, Shanghai 200241, People's Republic of China

Correspondence to: X. Wang (E-mail: xlwang@sjtu.edu.cn)

ABSTRACT: Tunable biodegradable polyurethanes (PUs) with favorable mechanical properties were synthesized from 1,6-hexamelthylene diisocyanate (HDI) as the hard segment, poly(ε-caprolactone) (PCL) as the soft segment, and L-cystine ester as chain extender. The structure of PUs was confirmed by FTIR and ^{1}H-NMR. The results of differential scanning calorimeter, thermogravimetric analysis, dynamic mechanical analysis, and tensile test revealed that the thermal and mechanical properties of PUs were strongly influenced by the molecular weight of soft segment PCL. In the presence of glutathione, the disulfide group cleaved into thiols, realizing the PUs degraded and the molecular weight decreased. For PU [550], it remained only 50% of the original M_w. Evaluation of cell viability demonstrated the nontoxicity of the PUs, which facilitated their potential in biomedical applications. © 2012 Wiley Periodicals, Inc. J. Appl. Polym. Sci. 128: 4047–4057, 2013

KEYWORDS: biodegradable; polyurethanes; elastomers

Received 21 May 2012; accepted 19 September 2012; published online 17 October 2012
DOI: 10.1002/app.38613

INTRODUCTION

Amino acid-based polymers, as a novel type of synthetic biomaterial, have sparked considerable research interest over the last decade, leading to a rich set of various applications being explored.[1–3] According to structural configuration, these materials could be classified into several subcategories: synthetic polymers with amino acid side chains, copolymers of amino acid and nonamino acid monomer, block copolymers containing peptides or poly(amino acid) blocks, and pseudo-poly(amino acid)s.[4] Because of their unfavorable physical mechanical properties, poly(amino acid)s thus evolved into the materials, which were known as "nonpeptide amino acid-based polymers" or as "amino-acid-derived polymers with modified backbones," which improved engineering properties and expanded biomedical applications.[5] L-Cysteine, as a kind of natural amino acid-containing thiol group, could dimerize into cystine through forming disulfide group as a bridge. When in a reductive environment, the cystine could regenerate into cysteine. The reversible transformation through disulfide-thiol was universal in cells. This feature facilitated its potential of adopted as a building block for the design of biodegradable polymers.

Among the biodegradable materials, polyurethane (PU) has enjoyed an extensive popularity for a long history, owing to its microseparated structure of alternating soft and hard segment, which contribute to the excellent mechanical properties and favorable biocompatibility,[6,7] manifesting itself in a wide variety of applications in implantable devices such as part of the drug administration systems,[8,9] artificial blood vessels,[10,11] heart valves,[12,13] nucleus prosthesis for artificial intervertebral disk,[14,15] and other tissue engineering materials.[16,17]

Numerous articles and reviews have reported novel PUs of different degradation mechanisms, of which much importance was attached to use hydrolyzable linkages, especially to adopt aliphatic polyesters as the soft segment, of which most commonly available are poly(ethylene glycol) (PEG) and poly(ε-caprolactone) (PCL).[18,19] The subset of these materials containing PCL soft segment possessed particularly high moduli and ultimate tensile stress and moderate degradation rate *in vitro*, whereas PEGs-containing PUs showed poorer mechanical properties being difficult to form into the proper structure and with significantly higher degradation rate. To copolymerize these two could incorporate the advantages of each material, but inevitably conduced to complexity and uncontrollability.[20] Alternatively, de Paz[21] introduced disulfide bond into PUs, which commonly used for target-responsive system and demonstrated its preferable biodegradability. In our previous research, disulfide-

Applied Polymer SCIENCE

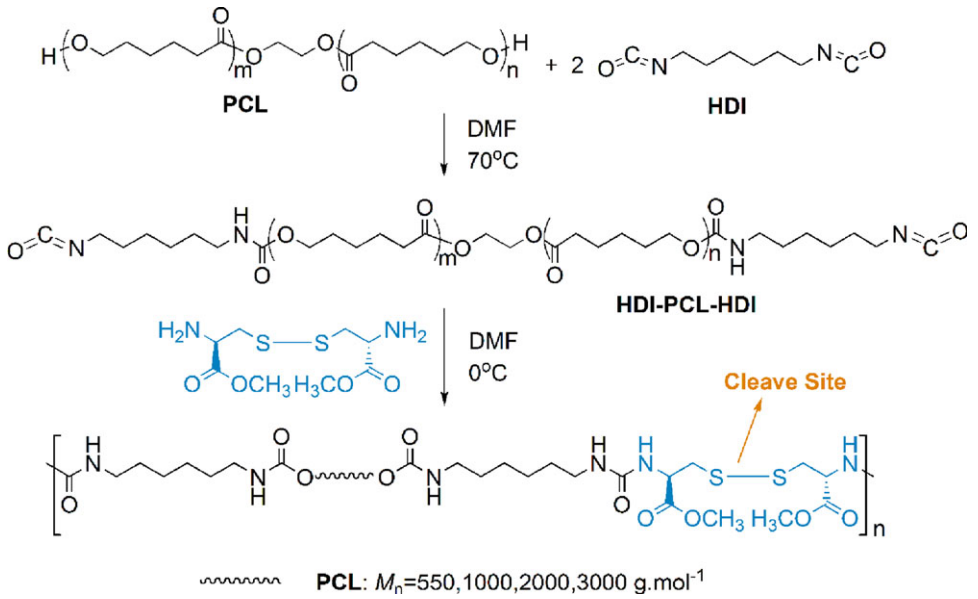

Scheme 1. Synthesis route of polyurethanes. [Color figure can be viewed in the online issue, which is available at wileyonlinelibrary.com.]

containing PUs based on 4,4′-dicyclohecylmethane diisocyanate (HMDI) and L-cystine had been proved to be biodegradable and biocompatible.[22]

In this work, we introduced cystine dimethyl ester as chain extender, which contained disulfide groups to serve as the degradable part. Aliphatic 1,6-hexamethylene diisocyanate (HDI) was selected as hard segment for its relatively low cytotoxicity among the diisocyanate and more universally used in the preparation of biomedical PUs. Compared to HMDI, HDI had a more flexible molecule chain, which might lead to higher reactive activity in preparation and degradation process. Here, PCL was used as soft segment for its excellent mechanical properties and favorable biocompatibility. Furthermore, the influence of molecular weight of PCL to the structures and properties of PUs was systemically investigated. Glutathione (GSH) exists in reduced and oxidized (glutathione disulfide, GSSG) states, where the GSH/GSSG system is the major redox couple in animal cells.[23] When in the presence of reduced GSH, disulfide bond in the hard segment of PUs was ready to cleave into thiols, which realize the PUs biodegradable.

EXPERIMENTAL

Materials

HDI was supplied by BASF. L-Cystine dimethyl ester dihydrochloride was purchased from Shanghai GL Biochem. Reduced GSH was provided by Beijing BioDee6 BioTech Corp. PCL with the number–average molecular weight M_n = 550, 1000, 2000, and 3000 g mol^{-1}, triethyl amine, dimethyl formamide (DMF), absolute ethanol (C_2H_5OH), absolute diethyl ether ($C_2H_5OC_2H_5$), calcium hydride (CaH_2), and dibutyltin dilaurate (DBTDL) were commercially obtained from Sinopharm Chemical Reagent.

Preparation of PUs

Pretreatment of Raw Materials. The polymerization reactions were performed via a standard, two-step reaction procedure, in the absence of humidity under an inert atmosphere, with the synthesis route as outlined in Scheme 1. All glassware was heated overnight at 102°C before use and, after assembly, was further heated under vacuum to eliminate the surface moisture. HDI was stored at 4°C and used as received. Treated as usual, DMF was dried with freshly powdered calcium hydride (CaH_2) and distillated under reduced pressure, storing over molecular sieves in a desiccator for not more than a week before use. The other reactants and reagents for the polymerization were dried extensively so as to minimize the traces of water as far as possible and stored in a desiccator under inert atmosphere until required.

Synthesis of PUs. PCL was introduced into a four-necked reaction kettle equipped with mechanical stirrer, heating mantle, reflux condenser, dropping funnel, and nitrogen inlet and outlet. The system was treated with three cycles of vacuum-nitrogen before the addition, via cannula, of anhydrous DMF (5 mL). The mixture was stirred to homogenization, and the HDI was added, followed by the catalyst DBTDL (one drop). The prepolymerization proceeded at 70°C for 2 h under an inert atmosphere with the presence of nitrogen and absence of humidity. The temperature was subsequently lowered to 0°C for the subsequent reaction.

In the second procedure, amino acid salt (L-cystine dimethyl ester dihydrochloride) was fully dissolved in DMF (10 mL) via ultrasonic vibration, and then the organic base (triethyl amine) was added into the reaction system. The neutralization product, L-cystine dimethyl ester, which could be adopted as chain extender, resided in its DMF solution after filtration. Sequentially, the filtrate was diluted with extra DMF (30 mL) and added into the reaction flask, dropwise. The polymerization proceeded at 0°C for 2 h and was allowed to recover to 25°C for two more hours. Dibutyl amine (0.05 mL) was used to cap the isocyanate residuals at the end of the macromolecule chains, and the mixture was stirred for another 30 min. The solution was added

Table I. Proportions of Raw Materials for Polyurethanes

	PCL			HDI		L-Cys	
PU	M_n (g·mol^{-1})	n (mmol)	m (g)	n (mmol)	m (g)	n (mmol)	m (g)
PU [550]	550	5.5	3.025	11	1.850	5.5	1.877
PU [1000]	1000	4	4	8	1.346	4	1.365
PU [2000]	2000	2.5	5	5	0.841	2.5	0.853
PU [3000]	3000	1.8	5.4	3.6	0.605	1.8	0.614

dropwise into diethyl ether, where the polymer precipitated immediately. The pure polymer (white solid) was dried under vacuum for 24 h and stored in a desiccator.

The proportions of raw materials were listed in Table I.

Characterizations

ATR–FTIR Spectroscopy. Attenuated total reflectance Fourier transform infrared (ATR–FTIR) spectra were recorded on a Perkin-Elmer 100 FTIR spectrometer equipped with an ATR accessory using Ge crystal, four scans collected for each sample with a resolution of 2 cm^{-1}.

NMRSpectroscopy. ^{1}H-NMR and ^{13}C-NMR spectra were obtained on MERCURYplus 400 spectrometer (Varian, CA) at 25°C, with deuterated DMSO as solvent. Chemical shifts (δ) are reported as parts per million (ppm) downfield from tetramethylsilane.

Molecular Weight Determination. Gel permeation chromatography (GPC) analyses were performed on a TOSOH EcoSEC HLC-8320GPC system with DMF as the mobile phase. All molecular weights were relative to polymethylmethacrylate standards.

Differential Scanning Calorimeter. The thermal behavior of the poly(urea-urethane)s was examined by differential scanning calorimeter (DSC), TA Instrument Q2000 under nitrogen atmosphere. Samples of 4–6 mg were heated from 40 to 120°C at a rate of 20°C min^{-1} and held at 120°C for 10 min to eliminate thermal history. The samples melt were then cooled to −80°C at 20°C min^{-1} and kept isothermal for 3 min, followed by heat to 120°C at 10°C min^{-1}. The T_g values were taken as the midpoints of the transition zones.

Thermogravimetric Analysis. Thermogravimetric analysis (TGA) was investigated by TA Instrument Q5000IR at a heating rate of 20°C min^{-1} in the range of 40–600°C under nitrogen atmosphere (flow rate 40 mLmin^{-1}).

Tensile Test. Tensile dumb-bell specimens were cut from the 1-mm-thick sheets and tested using an Instron 4465 tensile tester, according to ASTMD638-89, at a crosshead speed of 50 mmmin^{-1}. Tests were performed in a temperature and humidity-controlled environment after sample preconditioning for at least 48 h.

Dynamic Mechanical Analysis. To determine the storage modulus (E') and the tangent of phase lag (tan δ) of the PUs, dynamic mechanical analysis (DMTA) were performed on a NETZSCH DMA242 C in film tension mode at 1 Hz during a temperature ramp of 3°C min^{-1} starting at −80°C (to determine the mechanical glass transition temperature) up to the temperature limit at which the elastic modulus was experimentally inaccessible. Samples were punched into a rectangle of 30 mm length, 6 mm width, and 0.5 mm thickness.

Scanning Electron Microscope. The surface morphology of the PU films was studied with a field emission scanning electron microscope (SEM) JSM-7401 F from JEOL, Japan. To avoid charging of the surface for the highly nonconductive polymer, a conductive layer of gold about 5 nm was coated onto the PU samples.

Biodegradation of PUs with Glutathione

Preparation of Polymer Disks. PU films of each polymer studied were prepared by solution casting. The powders were dissolved in DMF at a concentration of 15% w/v to form a clear solution. The polymer solutions were poured into polytetrafluoroethylene-casting dishes and dried at room temperature until most of the solvent's removal, followed by vacuum drying for another 48 h to eliminate residual solvent. The PU films were then punched into disk (15 mm of diameter) pieces, ∼50 ± 5 mg, three samples each polymer studied, which were purified by ethanol and dried at 37°C for 48 h.

Biodegradation Conditions. Each polymer disk piece was submerged in a reduced GSH solution (0.1 *M*, 10 mL) at pH 7.02. A nitrogen flow was passed through the solution for 5 min, and the vial was then sealed and heated at 37°C for an exact period of time. The degradation experiments were quenched by alkylation of the free thiol groups generated to stabilize the degraded polymer fragments.

Quenched Degradation Experiments. The vial content was poured into a flask provided with a stirring bar. Phosphate-buffered solution (PBS; pH = 8.0 and 10 mL) and iodoacetic acid (0.1860 g, 1 mmol) were added sequentially. The mixture was stirred at 25°C for 1 h. The liquid phase was eliminated, and the films were washed with distilled water (3 × 10 mL) and then dried. The molecular weights of the degraded polymers were studied by GPC.

Cell Viability Test

WST-1 assay was adopted to measure cell viability.[24] PU disks were placed into a 24-well flat culture plate. A human umbilical vein endothelial cells' (HUVECs) suspension (50,000 mL^{-1}, 500 μL) was transferred into each well and cultured for 24 and 48 h. Sterilized PBS (0.01 *M*, pH 7.4, 500 μL) was used to substitute the culture medium, before adding 1/10 (v/v) of WST-1 reagent. The cells were incubated for another 1 h, after which the

supernatant was transferred into a 96-well flat plate with 150 μL each well. The absorbance at 450 nm was measured and recorded by a microplate reader (Model 680, Bio-Rad). Meanwhile, the cells cultured on glass slides at the same time intervals were used as controls (100% of viability), and background absorbance was measured in the culture medium without cells.

RESULTS AND DISCUSSION

Synthesis and Characterizations of PUs

In an effort to develop elastomeric, biocompatible, and biodegradable polyurethanes (PUs) applicable in bioengineering, amino acid esters were adopted as chain extender, with PCL as the soft segment and HDI as the hard segment. The reaction of PCL with excess amounts of HDI led to NCO-terminated PU prepolymers, which subsequently coupled with amino acid esters to prepare PUs, characterized by conventional spectroscopic methods. The structures of PUs were examined by ATR–FTIR and ^{1}H-NMR. The assignments of characteristic groups and protons in the polymers were provided in Figures 1 and 2.

Attenuated Total Reflectance-Fourier Transform Infrared. Generally, in attenuated total reflectance Fourier transform infrared (ATR–FTIR) spectra, the PUs presented quite similar signals, indicating no great differences in structure among them. Actually, the concerned sulfur-containing groups like S—S and S—CH_2 often expressed indistinctive absorption strength, thus easy to be outweighed by other overwhelmed peaks and difficult to be recognized clearly. Take PU [550] in Figure 1 for example to assign the peaks to corresponding groups in PUs. It could be seen that the peaks appeared at 3320 and 1549 cm^{-1} were stretching and deformation vibration of —NH— in urethane and urea group, of which the carbonyl stretching vibration was split into peaks 1725 and 1628 cm^{-1}, with N—C—O and CO—O asymmetrical stretching vibration at 1237 and 1162 cm^{-1}, respectively. The peak at 1101 cm^{-1} was asymmetric stretching vibration of O—C—C band in PCL. Methyl and methylene stretching vibration could be found between 2863 and 2938 cm^{-1}. Obviously, here, the PU with higher molecular weight of PCL, and thus higher proportion of soft segment, showed more intensive peaks attributed to ester group as well as the signals of urethane group was relatively weakened correspondingly.

Nuclear Magnetic Resonance. ^{1}H-nuclear magnetic resonance (NMR) and ^{13}C-NMR spectra of the PUs were also in accordance with the proposed structures, and PU[550] was assigned as an example in Figure 2. Especially in Figure 2(a), the peak noted in the parentheses (i) was possibly related to the caprolactone units adjacent to urethane group forming in the polymerization.

Gel Permeation Chromatography. The yields and molecular weights (number–average M_n and weight–average M_w) of the PUs were listed in Table II. It could be observed that the PUs all exhibited relatively high-molecular weights, facilitating their applications as biomaterial. As is well known in the PU's preparation, the combination of diisocyanate with diol or diamine during the process of prepolymerization and chain extending was universally considered as a nucleophilic addition reaction.

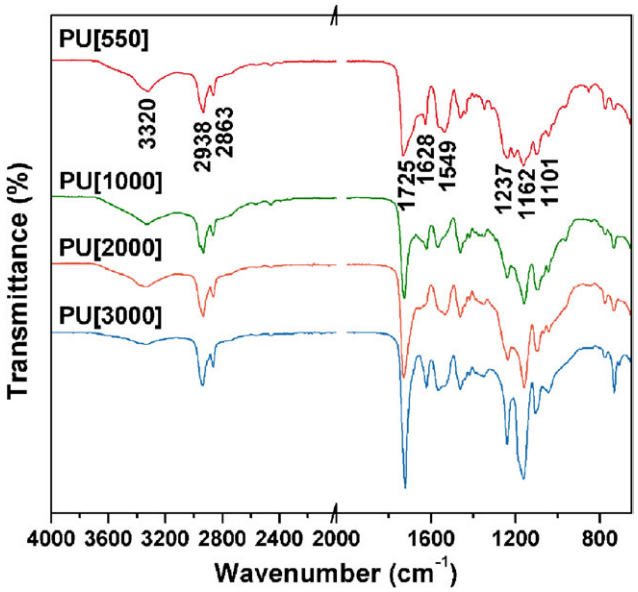

Figure 1. ATR–FTIR spectra of polyurethanes. [Color figure can be viewed in the online issue, which is available at wileyonlinelibrary.com.]

The molecular weight of PU thus keenly depended on that of prepolymer and its polymerization degree through chain extending, of which the two aspects should be interacted in a reciprocal relationship for each other. Evidently, PCL of higher molecular weight could provide the polymerization unit with longer chains, which inevitably exhibited lower reactivity for polymerization. Moreover, from the results here, it could be concluded that compared to the superiority in reactivity for smaller prepolymer, the molecular weight of reactive unit turned out to be the dominance in forming macromolecules.

Thermal Analysis

Differential Scanning Calorimeter. The phase behavior of the synthesized PUs was assessed with differential scanning calorimeter (DSC). The reversing heat flow versus temperature curves were displayed in Figure 3, showing the glass transition temperature (T_g), which was defined as the mid-point of the transition and the melting process. The thermal properties of the PUs were correspondingly listed in Table III.

As expected, the T_g of the PUs decreased with increasing soft segment molecular weight, indicating increasing phase separation. Accordingly, the increased phase mixing at low-soft segment molecular weight might result from more intensive disruption of hard segment or increased chemical compatibility between the HDI and cystine containing hard segment and low-molecular weight polyester soft segment.

It was worthwhile to notice that compared to the PUs of low-molecular weight soft segment, PU [2000] and PU [3000] also exhibited soft segment crystallization with the crystal melt temperature rising as PCL molecular weight was increased, providing further evidence of increased phase separation. In addition, the percent crystallinity of the soft segment of PUs was calculated assuming an enthalpy of fusion of 135.4 J g^{-1} for 100% crystalline PCL as determined by melting point depression of

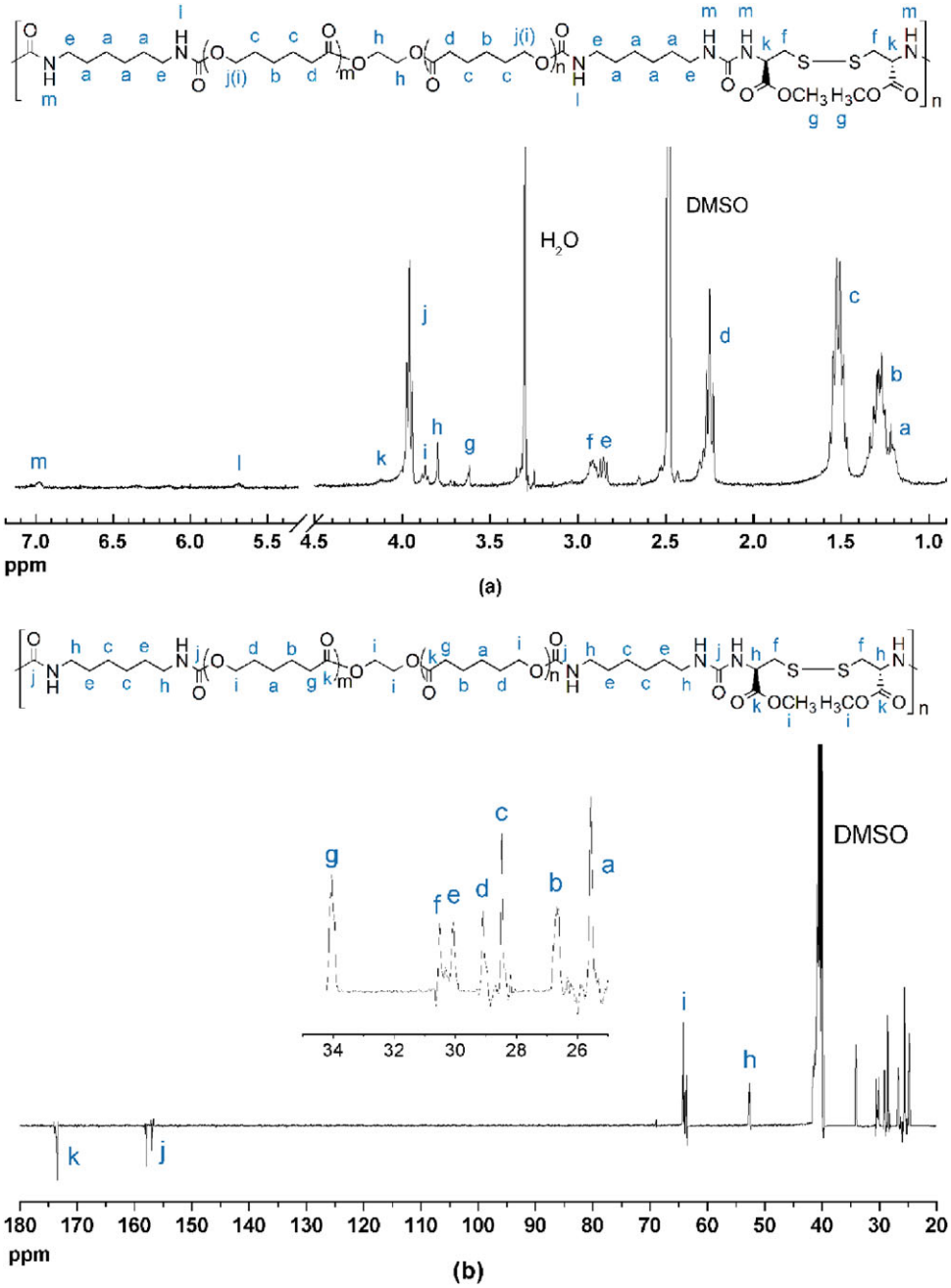

Figure 2. NMR spectra of PU[550]: (a) ^{1}H-NMR; (b) ^{13}C-NMR. [Color figure can be viewed in the online issue, which is available at wileyonlinelibrary.com.]

PCL with ethyl benzoate.[25] This performance of soft segment crystallization was similar to those noted by other researchers that a PCL molecular weight of 2000–3000 was necessary for crystallization.[26,27]

Thermogravimetric Analysis. The thermal stability of the prepared polymers was evaluated by thermogravimetric analysis (TGA), with the results collected in Table IV and Figure 4. As it conveyed, the thermal decomposition of these PUs involved two overlapping steps, which was distinguishable from TGA curves. The onset decomposition temperature of PUs showed a good

Table II. Yields and Average Molecular Weights by GPC

PU	Yield (%)	M_n (g mol^{-1})	M_w (g mol^{-1})	PDI (M_w/M_n)
PU [550]	94	20,499	47,842	2.3
PU [1000]	91	26,978	56,655	2.1
PU [2000]	86	25,902	62,165	2.4
PU [3000]	88	28,618	68,685	2.4

Applied Polymer SCIENCE

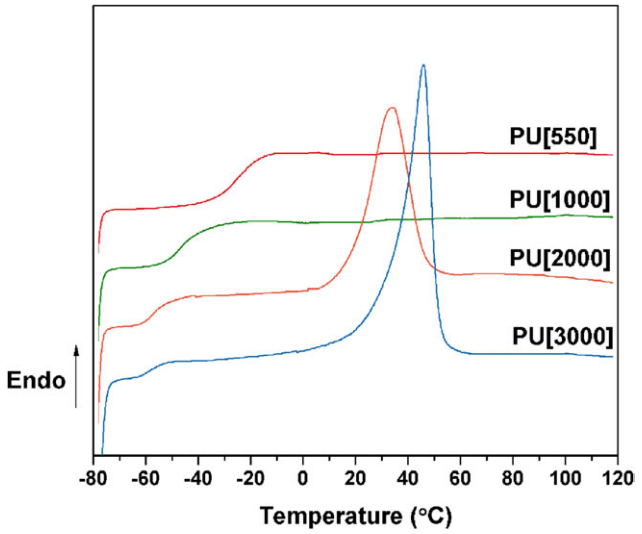

Figure 3. DSC curves of polyurethanes. [Color figure can be viewed in the online issue, which is available at wileyonlinelibrary.com.]

coincidence with the increasing molecular weight of PCL, and thus the weight loss at the first stage was correspondingly decreased as well as that of the second stage increased. It is widely accepted that the thermal decomposition of PU usually started at the hard segment indicating the first stage in the curve, here possibly related to the breakage of methoxyl group and simple depolymerization of urethane and disulfide bond, whereas the second stage was often generated by the cracking of soft segment itself at a higher temperature.

Mechanical Properties

Tensile Test. Stress–strain curves for the PCL-based PUs were shown in Figure 5. In agreement with DSC results, the shape of the curves for PU [2000] and PU [3000] was typical for semicrystalline polymers above T_g, displaying a pronounced yield point followed by necking and drawing indicative of semicrystalline PUs,[26,28] whereas the completely amorphous PU [550] and PU [1000] exhibited a smooth transition in stress–strain behavior from the elastic to plastic deformation regions similar to lightly crosslinked rubbers.[27]

In detail, uniaxial stress–strain testing results were listed in Table V, derived from the curves in Figure 5, which indicated that ultimate tensile strength and strain all increased with increasing PCL molecular weight. This phenomenon was somewhat surprising, for segmented PU elastomers typically presented decreasing ultimate tensile stress and initial modulus with increasing soft segment content. Increasing PCL molecular

Table III. DSC Data of Polyurethanes

PU	T_g (°C)	T_m (°C)	ΔH_m (J g^{-1})	X_c (%)
PU [550]	−26.3	-	-	-
PU [1000]	−47.6	-	-	-
PU [2000]	−58.1	34.0	43.2	31.9
PU [3000]	−59.7	46.0	56.5	41.7

Table IV. Thermogravimetric Properties of Polyurethanes

PU	T_{d0} (°C)	T_{d1} (°C)	T_{d2} (°C)	ΔW_1 (%)	ΔW_2 (%)
PU [550]	186	211	343	20	74
PU [1000]	188	211	362	12	82
PU [2000]	192	216	376	8	89
PU [3000]	198	229	374	4	94

T_{d0}, onset of decomposition; T_{d1}, T_{d2}, decomposition temperatures measured at the first, second peak of the derivative curves; ΔW_1, ΔW_2 loss weight of the first, second decomposition step.

weight led to increasing PU molecular weight (Table II), and this might be expected to result in increasing tensile properties as observed. However, previous research had clearly pointed out that increasing total polymer molecular weight above 25,000 had little effect on resulting PU elastomer physical properties. Thus the essential cause for the trend noted here was not believed to be the increasing polymer molecular weight with PCL content, but other three aspects as follows. First, the lack of hard segment crystallization attributed to the asymmetric polarity of urea or urethane groups and large side chain containing chain extender reduced the ability of the hard segment to act as a reinforcing filler or physical crosslinking site. Second, the presence of soft segment crystallization at 2000 and 3000 molecular weight might have an overriding effect on the overall polymer tensile strength and stiffness, for the soft segment crystal structures could presumably act as physical crosslinks in a manner similar to that normally ascribed to the hard segment. Yen and Cheng[29] have reported that increased polyester soft segment (polybutylene adipate glycol) crystallinity with increased molecular weight resulted in both increased ultimate tensile strength and ultimate elongation as seen herein. Finally, the increasing degree of phase separation noted with increasing PCL content might also significantly impact the resultant tensile properties. Increasing phase separation has been found to lead to enhanced tensile properties for polyester-based PUs, and this phenomenon was believed to result from the increased hard domain cohesion from a phase-segregated morphology.[28] The importance of both soft segment crystallinity and phase separation was highlighted by relatively low-tensile properties of PU [550] weaker than the more phase-separated PU [1000], PU [2000], and PU [3000].

Dynamic Mechanical Analysis. The viscoelastic properties of the samples were studied by means of dynamic mechanical analysis (DMTA), which had become a classic method allowing the determination of different types of transitions, and relaxations to be detected for the height and position of the mechanical damping peaks were markedly affected by miscibility, intermolecular interaction, and morphology. The temperature dependence of storage modulus (E') and loss tangent (tan δ) was shown in Figure 6. Especially, in the log E' verses temperature curves, it was obviously observed that PU [550] and PU [1000] had a single phase structure, as shown by only one relaxation in the region below 0°C, attributed to glass transition. Samples PU [2000] and PU [3000] exhibited two thermal

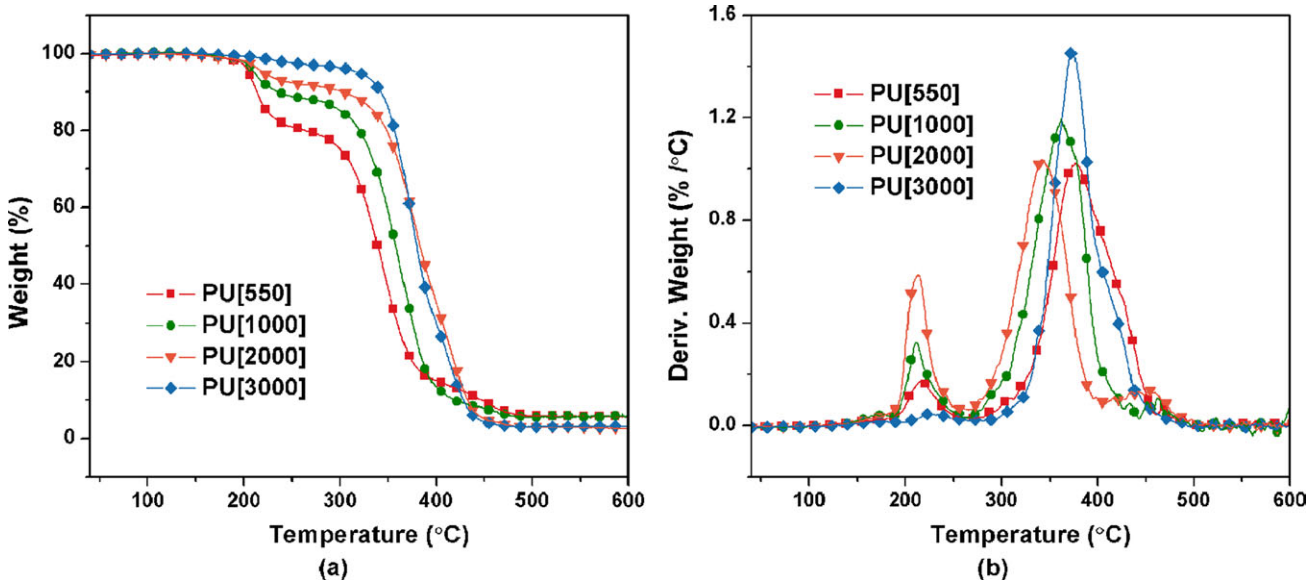

Figure 4. TGA curves of polyurethanes: (a) weight loss; (b) derivation of weight loss. [Color figure can be viewed in the online issue, which is available at wileyonlinelibrary.com.]

transitions, of which the low-temperature transition was related to the glass transition (T_g) as well as the higher temperature transition corresponding to the melting of the crystalline phase of soft segment (T_m). As it were, these results agreed quite well with that of DSC.

An investigation of the tan δ curves exhibited that the glass transition peak shifted to a lower temperature with an increase in the molecular weight of PCL chains, which was attributed to the expansion of phase separation accompanied with crystallization in PCL. The opposite trend had been observed for the position of the crystalline melting peak, which was shifted to a higher temperature with an increase in the crystalline content of PU [2000] to PU [3000]. Also, the range of the tan δ peaks, an indication of phase separation, displayed an agreement with the performance analyzed earlier. In PU [550] and PU [1000], the properties of soft segment and hard segment were closer to each other, and they formed less phase separation and exhibited sharper peaks, whereas crystallized PU [2000] and PU [3000] had a more phase separation and exhibited wider temperature range of tan δ peaks.

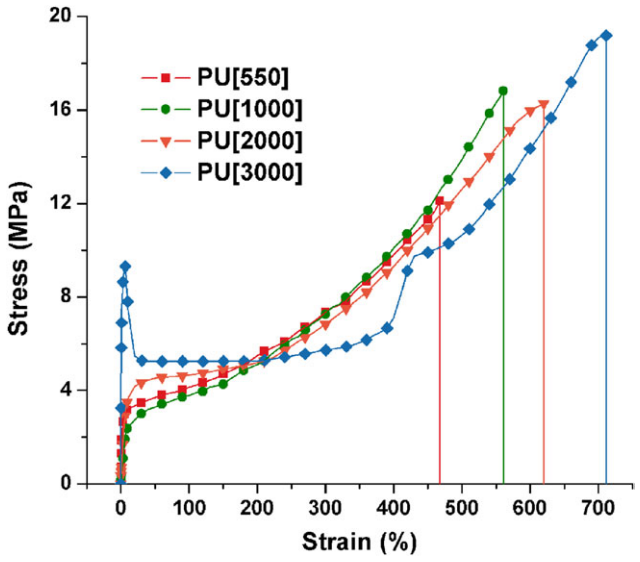

Figure 5. Stress–strain curves of polyurethanes. [Color figure can be viewed in the online issue, which is available at wileyonlinelibrary.com.]

Biodegradation of PUs

In vitro degradation studies under conditions (at 37°C and pH 7.02), the behaviors of the polyurethanes (PUs) were thoroughly investigated. As mentioned earlier, that disulfide bonds were prone to rapid cleavage under a reductive environment through the fast and readily reversible thioldisulfide exchange reactions, the same mechanism degradation pathway of L-cystine-based PUs was shown in Scheme 2.[21] The degraded polymeric fragments were subsequently stabilized by entrapping the newly generated free thiol as carboxymethyl thioether by treatment of iodoacetic acid in PBS buffer at pH 8.0, before being studied.

No measurable mass loss for the sample films about a month period was observed as well as free of generating products soluble in the incubation media. When the degradation test was prolonged, PU samples sharply decreased in mechanical

Table V. Tensile Properties of Polyurethanes

PU	Tensile strength (MPa)	Elongation at break (%)
PU [550]	12.1	468
PU [1000]	16.9	561
PU [2000]	16.3	620
PU [3000]	19.4	701

Applied Polymer SCIENCE

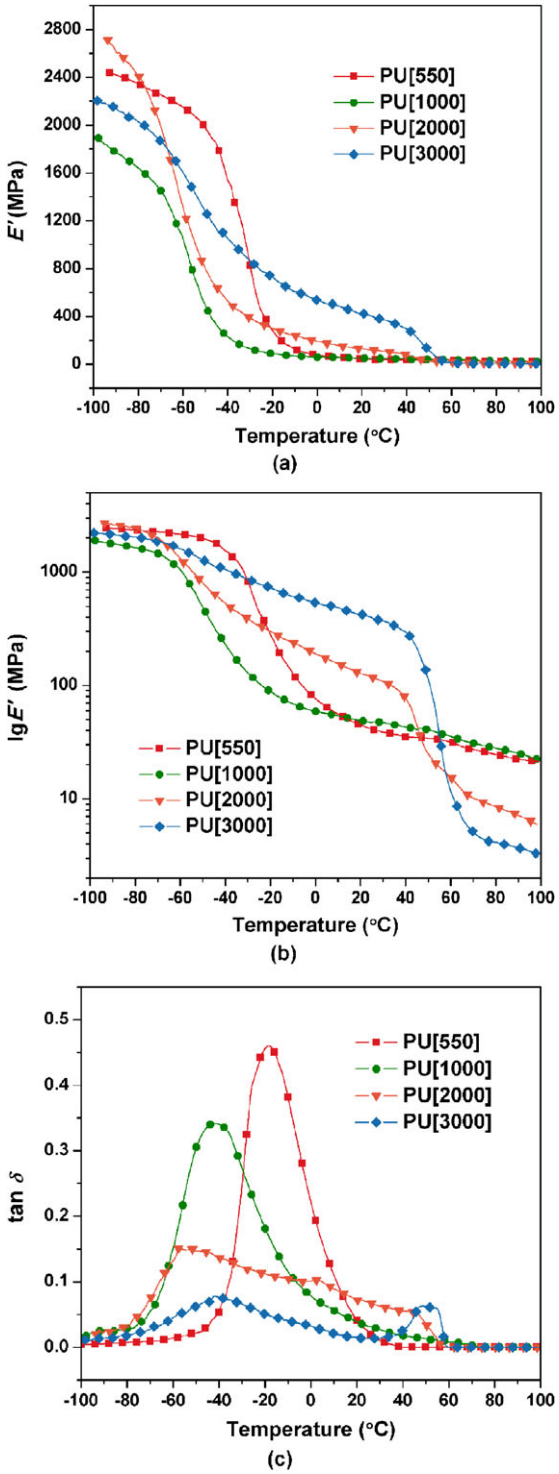

Figure 6. DMTA curves of polyurethanes: (a) storage modulus (E'); (b) log E'; (c) tan δ. [Color figure can be viewed in the online issue, which is available at wileyonlinelibrary.com.]

properties and even collapse, which made their weights hard to be accurately measured. This phenomenon might be as a result of decreasing molecular weight. As was expected, the GSH-responsive degradation was attributed to the disulfide bond introduced into PUs as chain extender through L-cystine, which was susceptible to the existence of GSH and readily cleaved into sulfydryl in a short while. The biodegradation process of these PUs was monitored by GPC to determine the changes in molecular weight undergoing throughout the incubation period. The evolution of weight–average molecular weights (M_w) was graphed in Figure 7.

The decomposition behavior of the PUs was all present with a rapid decrease in molecular weight during the first 4 days of incubation, followed by a second period in which degradation proceeds at a much lower rate. As it revealed as previous expectation, the degradation ability of PUs decreased with the increase of soft segment molecular weight, or rather, the decrease of degradable segment content.

Admittedly, the content of disulfide groups of polymer was assumed to be a key parameter in their kinetics. Therewithal, the remaining molecular weight of PUs PU[M] (M = 550, 1000, 2000, and 3000) after 30 days was increasing in this order, but not exactly correspondent to the content of L-cystine (23%, 17%, 10%, and 7%, wt). According to the previous analysis of PU structures, it was well reasonable to deduce that besides their chemical composition, the degradation behaviors of PUs were closely affected by the physical properties like conformation and configuration, as macromolecules. Here, in PU [550], the degradation rate could be favorably maintained during the whole process, while it was sharply reduced in PU [1000]. Furthermore, in PU [2000] and PU [3000], the degradation rate almost kept constant after the initial 4 days, possibly due to the weak affinity to the ambient surroundings of regularly packed polymer chains, especially containing crystallized regions. Compared to the PEG-contained PUs previously tested, these PCL-based ones showed a little decline in degradation velocity. Generally, the degradation behavior of these PUs could be considered as surface degradation, which was significantly affected by the surface property of the materials. It is widely known that PEG segment had an excellent hydrophilicity and was more ready to get an access to the incubation media, which might account for its superiority in degradability. Nevertheless, it was worthwhile to point out that the melting point of PU [2000] and PU [3000] was around 40°C, just a little bit higher than the normal temperature of the human body at 37°C, which made itself quite possible to facilitate drug-delivery system as temperature-sensitive carrier.[30]

To extend the process into more comprehensive illustration, ^{1}H-NMR was adopted to examine the chemical shift of hydrogen before and after degradation, coupled with SEM photographs studied for surface morphology, exhibited in Figures 8 and 9, respectively.

The SEM analysis of samples before and after degradation provided valuable information directly. The disk had a flat surface initially, and numerous holes were born out upon degradation, indicating that the materials underwent attack in the bulk. It was assumed that small size of tripetide GSH facilitated its dispersion into the polymer disk all along the trials with degradation effects not only over the surface of the polymer disks but also in their inner part. A large amount of material appeared attached on the surface in the form of granules; this was thought to comprise the nonsoluble fragments generated upon

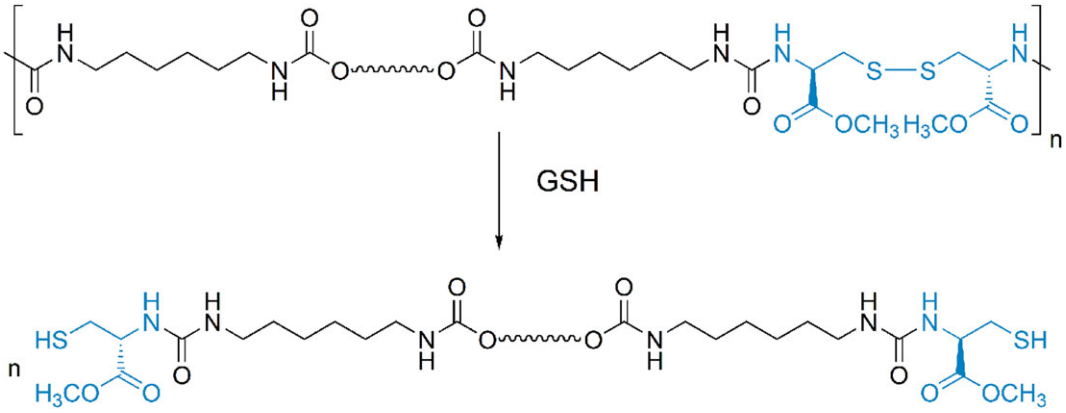

Scheme 2. Degradation of L-cystine-based polyurethanes mediated by reduced glutathione. [Color figure can be viewed in the online issue, which is available at wileyonlinelibrary.com.]

enzymosis. It seemed, therefore, that no weight loss was observed, because the degraded material was not released into the incubation medium.

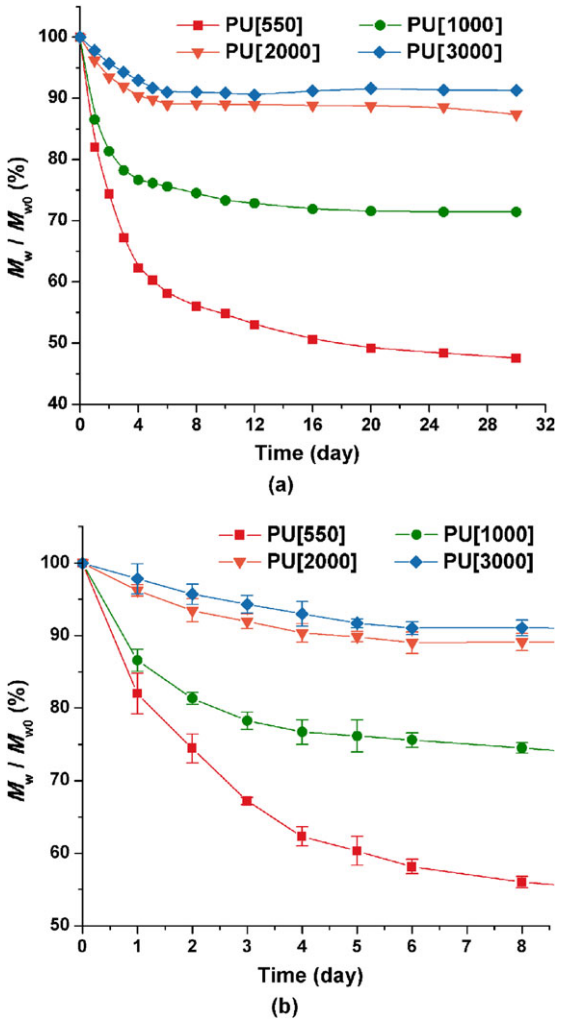

Figure 7. Molecular weight of polyurethanes in glutathione-responsive degradation: (a) 0–30 days; (b) 0–8 days. [Color figure can be viewed in the online issue, which is available at wileyonlinelibrary.com.]

Table VI summarized the properties of PUs with HDI or HMDI as hard segment. For the PUs with the same soft segment, PU [1000] and PU [2000] had a little higher molecular weight than PCL1000-HMDI and PCL2000-HMDI, respectively, which might be due to its more flexible chain and less steric hindrance in HDI and thus a little higher reactivity. Furthermore, PU [2000] was partial crystallized while PCL2000-HMDI was totally amorphous, which should benefit from the regularity of HDI. Therefore, the crystallized PCL segment in PU [2000] led to higher tensile strength. Just because of more regularity of HDI-contained PUs, in degradation test, they showed a little slower degradation rate.

Cell Viability Studies

WST-1 assay was carried out to evaluate the biocompatibility of these PUs, on which the HUVEC cell was cultured, and the cell growth denoted as viability was detected. The majority of cells had undergone proliferation during 2-day incubation, as Figure 10 showed. Compared to glass substrate as control sample, no significant difference of cell viability was observed for this series of PUs, and furthermore, the cells could be benignly proliferated in 2 days. Both the PCL and cell membrane had ester groups in their structures, from which PCL might benefit for its biocompatibility. In Figure 10, the PU with higher molecular weight of PCL segment revealed better appropriateness for cell growth,

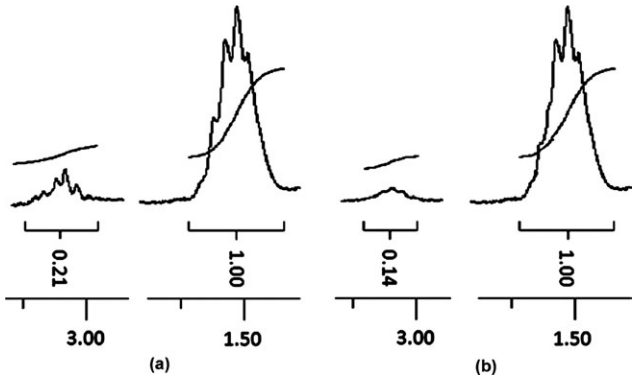

Figure 8. ^{1}H-NMR spectra of PU[550] samples in biodegradation before (a) and after (b) incubation for 4 days.

Applied Polymer SCIENCE

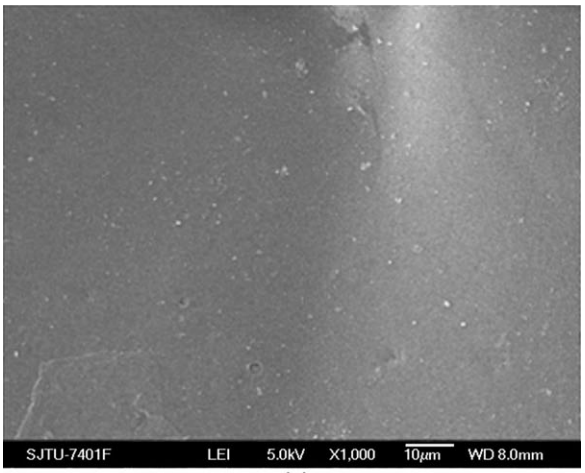

Figure 9. SEM micrographs in degradation: (a) PU[550] before incubation; (b) PU[550] after 4 days; (c) PU[2000] after 4 days.

because PCL soft segment might have more compatibility compared to the hard segment for its ester groups. Generally, the cell viability results of the PUs all demonstrated themselves of noncytotoxicity and biocompatibility.

Table VI. Properties of PCL-Containing Polyurethanes with HMDI or HDI as Hard Segment

PU	PU [1000]	PCL1000-HMDI	PU [2000]	PCL2000-HMDI
M_n	26,978	26,100	25,902	21,400
M_w	56,655	52,900	62,165	43,200
PDI	2.1	2.0	2.4	2.0
T_g (°C)	−47.6	−26.6	−58.1	−48.2
T_m (°C)	-	34.0	-	-
Tensile strength (MPa)	16.9	12.0	16.3	10.4
Elongation at break (%)	561	438	620	513
M_w/M_{w0} (8 days)	75	66	88	72

CONCLUSION

Tunable biodegradable PUs with favorable mechanical properties were synthesized from HDI as the hard segment, PCL as the soft segment, and L-cystine ester as chain extender. The structure, thermal, and mechanical properties of PUs were characterized with ATR–FTIR, ^{1}H-NMR, GPC, DSC, TGA, and tensile test, proved to be strongly influenced by the molecular weight of soft segment PCL.

The degradation behavior in the presence of GSH media of these PUs showed that PU [550] presented the best degradability for only remaining ~50% of the original M_w. With the increase in PCL molecular weight, the degradability gradually compromised due to the decreased content of disulfide group and well-organized structure, even crystallization. All the PUs were testified to be noncytotoxic and biocompatible.

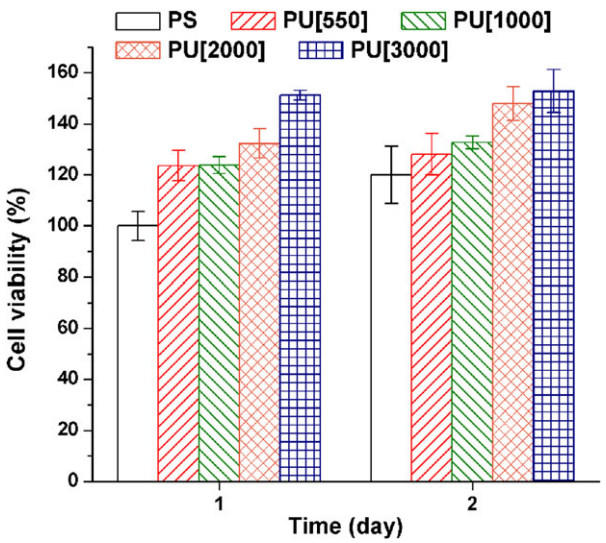

Figure 10. Cell viability on polyurethane surfaces.

REFERENCES

1. Farrar, D.; Ren, K.; Moon, W.; Wilson, W. L.; West, J. E.; Yu, S. M. *Adv. Mater.* **2011**, *23*, 3954.
2. Obeid, R.; Scholz, C. *Biomacromolecules* **2011**, *12*, 3797.
3. Wang, L. L.; Wu, Y. X.; Xu, R. W.; Wu, G. Y.; Yang, W. T. *Chin. J. Polym. Sci.* **2008**, *26*, 381.
4. Kemnitzer, J.; Kohn, J. In Drug Targeting and Delivery, Handbook of Biodegradable Polymers; Domb, A. J., Kost, J., Wiseman, D. M., Eds.; Harwood Academic: Amsterdam, **1997**; p 251–272.
5. Panchene, J. P.; Kohn, J. In Principles of Tissue Engineering; Lanza, R. P., Langer, R., Chick, W. L., Eds.; Academic Press: California, **2000**; p 263–278.
6. Maki, D. G. In Infections Associated with Indwelling Devices; Bisno, A. L., Waldvogel, F. A.Ed.; ASM: Washington DC, **1989**; p 161–177.
7. Zhang, X. Q.; Jiang, X.; Li, J. H.; Liu, J.; Tan, H.; Zhong, Y. P.; Fu, Q. *Chin. J. Polym. Sci.* **2008**, *26*, 203.
8. Zhou, L. J.; Yu, L. Q.; Ding, M. M.; Li, J. H.; Tan, H.; Wang Z. G.; Fu, Q. *Macromolecules* **2011**, *44*, 857.
9. Caon, T.; Zanetti-Ramos, B. G.; Lemos-Senna, E.; Cloutet, E.; Cramail, H.; Borsali, R.; Soldi, V.; Simoes, C. M. O. *J. Nanopart. Res.* **2009**, *12*, 1655.
10. Doi, K.; Matsuda, T. *J. Biomed. Mater. Res.* **1997**, *37*, 573.
11. Meyer, E. P.; Beer, G. M.; Lang, A.; Manestar, M.; Krucker, T.; Meier, S.; Mihic-Probst, D.; Groscurth, P. *Clin. Anat.* **2007**, *20*, 448.
12. Alferiev, I.; Stachelek, S. J.; Lu, Z. B.; Fu, A. L.; Sellaro, T. L.; Connolly, J. M.; Bianco, R. W.; Sacks, M. S.; Levy, R. J. *J. Biomed. Mater. Res. A* **2003**, *66*, 385.
13. Han, D. K.; Park, K.; Park, K. D.; Ahn, K. D.; Kim, Y. H. *Artif. Organs* **2006**, *30*, 955.
14. Tsantrizos, A.; Ordway, N. R.; Myint, K.; Martz, E.; Yuan, H. *SAS J.* **2008**, *2*, 28.
15. Wang, J.; Xia, W.; Liu, K.; Tuo, X. *J. Appl. Polym. Sci.* **2011**, *121*, 1245.
16. Hofmann, A.; Ritz, U.; Verrier, S.; Eglin, D.; Alini, M.; Fuchs, S.; Kirkpatrick, C. J.; Rommens, P. M. *Biomaterials* **2008**, *29*, 4217.
17. Andrews, K. D.; Hunt, J. A.; Black, R. *Polym. Int.* **2008**, *57*, 203.
18. Hassan, M. K.; Mauritz, K. A.; Storey, R. F.; Wiggins, J. S. *J. Polym. Sci. A* **2006**, *44*, 2990.
19. Wang, W. S.; Ping, P.; Yu, H. J.; Chen, X. S.; Jing, X. B. *J. Polym. Sci. A* **2006**, *44*, 5505.
20. Yeganeh, H.; Jamshidi, H.; Jamshidi, S. *Polym. Int.* **2007**, *56*, 41.
21. De Paz, M. V.; Zamora, F.; Begines, B.; Ferris, C.; Galbis, J. A. *Biomacromolecules* **2010**, *11*, 269.
22. Lu, H.; Sun, P.; Zheng, Z.; Yao, X.; Wang, X. *Polym. Degrad. Stab.* **2012**, *97*, 661.
23. Wu, G.; Fang, Y. Z.; Yang, S.; Lupton, J. R.; Turner, N. D. *J. Nutr.* **2004**, *134*, 489.
24. Worle-Knirsch, J. M.; Pulskamp, K.; Krug, H. F. *Nano Lett.* **2006**, *6*, 1261.
25. Crescenzi, V.; Manzini, G.; Calzolari, G.; Borri, C. *Eur. Polym. J.* **1972**, *8*, 449.
26. van Bogart, J. W. C.; Gibson, P. E.; Cooper, S. L. *J. Polym. Sci. B* **1983**, *21*, 65.
27. Hepburn, C. Polyurethane Elastomer; Elsevier Applied Science: London, **1993**.
28. Foks, J.; Janik, H.; Russo, R. *Eur. Polym. J.* **1990**, *26*, 309.
29. Yen, M. S.; Cheng, K. L. *J. Appl. Polym. Sci.* **1994**, *52*, 1707.
30. Chen, Y.; Wang, R.; Zhou, J.; Fan, H.; Shi, B. *React. Funct. Polym.* **2011**, *71*, 525.